Conformational stabilities, infrared, and vibrational dichroism spectroscopy studies of tris(ethylenediamine) zinc (II) chloride

N. Norani · H. Rahemi · S. F. Tayyari · M. J. Riley

Abstract The conformational stabilities of the transition metal complex of Zn $(en)_3Cl_2$ were studied using density functional theory (DFT). Deformational potential energy profiles (PEPs), and pathways between the different isomeric conformational energies were calculated using DFT/B3LYP/6–31G. The relative conformational energies of $\Delta(\lambda\lambda\lambda)$, $\Delta(\lambda\lambda\delta)$, $\Delta(\lambda\delta\delta)$ and $\Delta(\delta\delta\delta)$ are 10.48, 7.08, 3.56, and 0.0 kcal/mol, respectively, which are small compared to the barrier heights for reversible phase transitions (49.56, 49.55, 49.52 kcal/mol, respectively). Frequency assignment was carried out by decomposing Fourier transform infrared (FTIR) spectra using Gaussian and Gaussview. The theoretical IR and vibrational dichroism spectroscopy (VCD) absorption spectra are presented for all conformations within the range of 400–3,500 cm^{-1}.
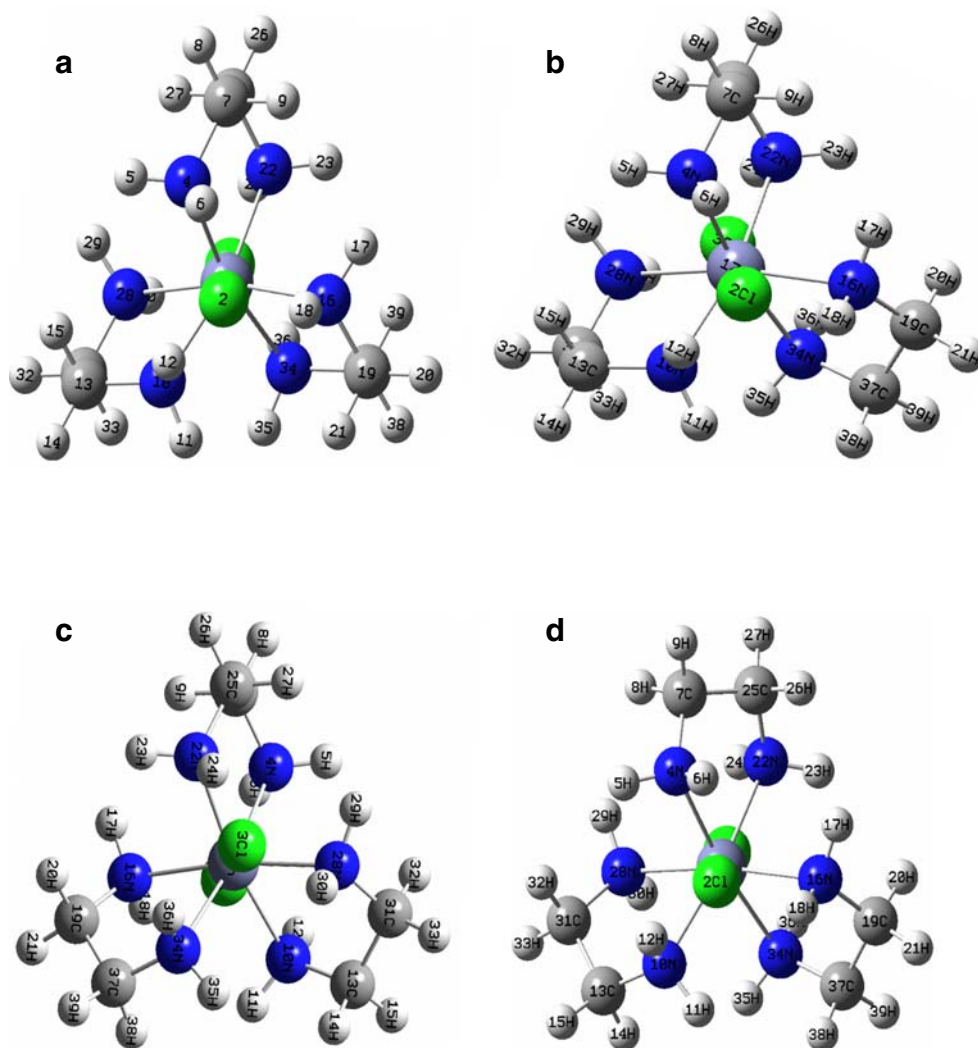
N. Norani
Payam-Noor University,
Urmia, Iran

H. Rahemi (✉)
Chemistry Department, Urmia University,
57159–165 Urmia, Iran
e-mail: hrahemi@yahoo.com

S. F. Tayyari
Chemistry Department, Ferdowsi University,
Mashhad 91775–1435, Iran

M. J. Riley
Chemistry Department, University of Queensland,
Brisbane, Queensland 4072, Australia

Introduction

Because transition metal complexes of the general form M $(en)_3^{n+}$ are ideal host lattices for single crystals, many studies have investigated their electron paramagnetic resonance (EPR), reversible phase transitions, and optical activities for electronic dichroism spectroscopy (ECD) and vibrational dichroism spectroscopy (VCD) [1–5].

A chiral ethylenediamine ligand of such a complex can take one of two enantiomeric conformations, and can exist in four conformational isomers, with the C–C bond being either nearly parallel (δ–form) or oblique (λ–form) to the C_3 axis of symmetry in the Λ–conformation—denoted by $\Lambda(\delta\delta\delta)$, $\Lambda(\delta\delta\lambda)$, $\Lambda(\delta\lambda\lambda)$ and $\Lambda(\lambda\lambda\lambda)$ [4, 6], which are degenerate with other enantiomers $\Delta(\lambda\lambda\lambda)$, $\Delta(\lambda\lambda\delta)$, $\Delta(\lambda\delta\delta)$ and $\Delta(\delta\delta\delta)$, respectively. Optimized structures of the Zn complexes are presented in Fig. 1. The reversible phase transitions can be explained by the conformational change of the complex site from D_3 to C_2 symmetry, e.g., the tris (ethane-1, 2-diamine) zinc (II) dinitrate phase transition occurs at 143 K [3].

Statistical information about the natural occurrence of enantiomers and isomers of crystalline structures of transition metal complexes of the form M(en)$_3^{n+}$ with M = Co, Ni, Ru, Zn, Tl, Cr, Cu, Rh, Cd, Ir, Os, V, Mn, Ga, Fe, Mg, and Ge, and with n = 2,3 has been reviewed in the literature [7]. The crystalline structure of these complexes were regenerated and checked for enantiomers and conformational isomers using the Platon computer program [8]. A total of 162 cases were examined and the number of occurrences of each conformation is as follows:

$\Delta(\delta\delta\delta)$	$\Delta(\delta\delta\lambda)$	$\Delta(\delta\lambda\lambda)$	$\Delta(\lambda\lambda\lambda)$	$\Lambda(\delta\delta\delta)$	$\Lambda(\delta\delta\lambda)$
6	10	10	44	65	17

$\Lambda(\delta\lambda\lambda)$	$\Lambda(\lambda\lambda\lambda)$
5	5

Fig. 1 The B3LYP/6-31G-optimized structure of Zn(en)₃Cl₂. **a** Δ(λλλ), **b** Δ(δλλ), **c** Δ(δδλ) and **d** Δ(δδδ) conformations, viewed along the C3 axis of symmetry

That there were 109 degenerate enantiomers Δ(λλλ) and Λ(δδδ) out of 162 occurrences is an indication of the low relative conformational energy of these isomers in the crystalline environment, and that these enantiomers were dominant over the statistically 3 to 1 favored intermediates Δ(δδδ), Δ(δδλ), Δ(δλλ), Λ(δδλ), Λ(δλλ) and Λ(λλλ).

In this work, we have employed computational studies as a complementary technique to aid in the understanding of the electronic and geometric structures of the zinc complexes. Specially, we performed some calculations on the relative stability and transition state pathways between various conformational isomers of the coordination com-

Table 1 Optimized bond lengths (Å) and bond angles (degrees) of tris(ethylenediamin)zinc(II)

	B3LYP/6–31G				
Variable	Δ(λλλ)	Δ(λλδ)	Δ(λδδ)	Δ(δδδ)	Experimental [18]
Bond length (Å)					
Zn-Cl	3.75	3.80	3.85	3.89	
Zn-N2	2.211	2.216	2.217	2.218	2.18 (1)
N5-CN5	1.48	1.48	1.48	1.48	1.48 (3)
CN3-CN6	1.51	1.52	1.52	1.53	1.47 (4)
Bond angle(°)					
N4-Zn-N6	96.45	96.36	96.36	96.32	96.2 (0.6)
Zn-N2-CN2	108.34	108.32	108.30	108.28	108.1 (1.5)
N1-CN1-CN4	109.47	109.65	109.71	109.72	108.4 (2.0)

pounds; their VCD and infrared (IR) absorption spectra are reported for closed shell Zn(en)$_3$Cl$_2$, d^{10}.

In agreement with theoretical energy calculations [9], the Λ(δδδ) isomer has been found to be the most abundant. More recently, however, it has been argued that hydrogen bonding [10] or crystal packing forces [11] may cause any of the four isomers to be the most stable. It has also been argued that entropy effects would cause the Λ(δδλ) isomer to have the lowest free energy [12].

Theoretical and computational developments

The computer program used was Gaussian 03W v.6.0 [13], and all calculations were carried out at the DFT level. The underlying theory is the Khon Sham approach to DFT [14], which uses a one-particle Schrödinger equation and performs self consistent field (SCF) procedures. The Vosko, Wilk and Nusair (VWN) formula [15] was used for local density approximation for general gradient approximation (GGA), Becke3 (B3) [16] as an exchange correction term and Lee-Yang-Parr (LYP) [17] as a correlation correction term, all with the B3LYP functional and with a reasonably large basis set of 6–31G.

Results

Transition state pathways

The DFT/B3LYP/6–31G optimizations of the complexes were performed with good accuracy; selected bond lengths and bond angles values are given in Table 1. Any small differences can be attributed to the comparison of free complex values to those of the solid state [18].

The Z–Matrix of Z(en)$_3$$^{n+}$ is constructed using X-ray data [3] and five dummy atoms, two along the C$_3$ axis and three along the C$_2$ axes for symmetry adjustments. The dihedral angles N–Zn–X (along the C$_3$ axes) –X (along the C$_2$ axes), H–N–Zn–X (D2), H–C–N–H (D5) and H–C–N–H (second) are optimized to obtain the conformational energies of each isomer. In order to carry out calculations on the conformational pathways, we found that variations of two dihedral angles, D2 and D5, are required. Other variables are designed in such a way that they adjust themselves with D2 and D5. Unfortunately, due to the instability of the complex in large deviations from optimized conformations, a grid scan run of both angles at the same time was not possible. Therefore, D2 and D5 were varied step by step (35 separate runs, single point calculations) to calculate conformational pathway energies. The pathway between different conformers of Z(en)$_3$$^{n+}$ in a crystalline environment is presented in Fig. 2. Conforma-
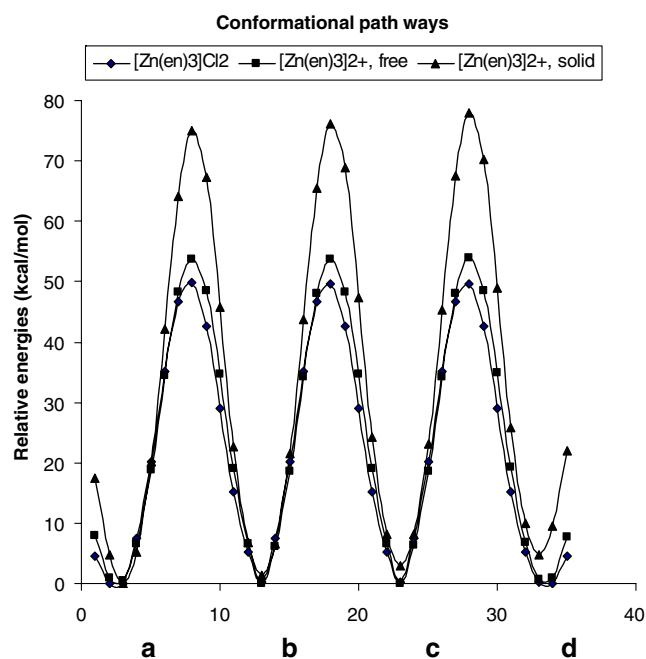

Conformational path ways
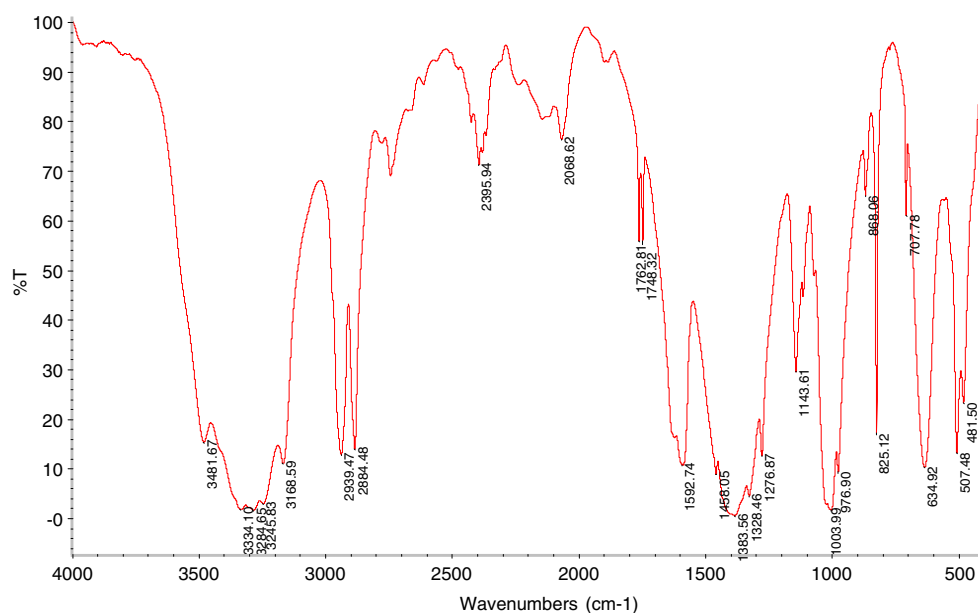
Fig. 2 Relative conformational pathways between isomers

tional energies and reversible phase transition barrier heights are listed in Table 2. The calculated order of stability of Z(en)$_3$$^{n+}$ isomers in the crystalline environment is Δ(λλλ)>Δ(λλδ)>Δ(λδδ)>Δ(δδδ), with a jump of about 1.5 kcal/mol between corresponding conformations. Therefore, the appearance of various isomers in different crystalline structures having high reversible phase transition barriers of about 77.93 kcal/mol is rather accidental.

Calculations were carried out for free ions in free space. The Z–matrices were constructed with 18 variables for Δ(λλλ) and Δ(δδδ), and with 36 variables for Δ(λλδ) and Δ(λδδ) conformers, and the geometry optimizations were repeated. Except D2 and D5, no bond lengths or bond angles changed significantly from one conformer to the next, therefore mean values were calculated and used in potential energy profile calculations (see Fig. 1, Table 1). The relative gas phase conformational energies of various isomers are the same within a fraction of a kilocalorie/mole,

Table 2 Relative conformational energies and barrier heights of [Zn (en)$_3$]Cl$_2$ and [Zn(en)$_3$]$^{2+}$ using X-ray data [3] and gas phase optimized geometry variables (in kcal/mol)

Conformer	[Zn(en)$_3$]$^{2+}$, solid	[Zn(en)$_3$]$^{2+}$, free	[Zn(en)$_3$]Cl$_2$
Δ(λλλ)	0.00	0.38	0.00
Barrier 1	74.91	53.82	49.76
Δ(λλδ)	1.42	0.00	0.12
Barrier 2	76.25	53.66	49.68
Δ(λδδ)	3.02	0.04	0.17
Barrier 3	77.90	53.86	49.68
Δ(δδδ)	4.74	0.65	0.12

Fig. 3 The Fourier transform infrared (FTIR) transmittance spectrum of solid $[Zn(en)_3]Cl_2$

and barrier heights compared to those of the solid state are low (53.86 kcal/mol). The conformational energies of Δ (δδλ) and Δ (δλλ) are lower than those of Δ (δδδ) and Δ (λλλ), giving them a bit more stability with which to meet the statistically (3:1) favored conformation.

The same calculations were also performed for the [Zn (en)$_3$]Cl$_2$ in free space. The results are given in Table 2 and Fig. 2. Comparison of Z(en)$_3^{n+}$ and [Zn(en)$_3$]Cl$_2$ shows that inclusion of the chlorine atoms lowers the barrier height by about 4 kcal/mol. The most stable conformer within a fraction of a kilocalorie/mole is Δ(λλλ).

IR and VCD spectra

Tris(ethylenediamine) zinc (II) chloride, $[Zn(en)_3]Cl_2$, was prepared by adding excess ethylenediamine to an aqueous solution of zinc chloride. When the product precipitated from solution upon addition of acetone, it was immediately filtered [19, 20] and dried. KBr tablets of $[Zn(en)_3]Cl_2$ are prepared and the FTIR spectrum in the 400–4,000 cm^{-1}

region (Fig. 3) was measured using an FT-IR Thermonicolet, Nexus-670 spectrophotometer. Calculation of the vibrational frequency spectrum of a nonlinear molecule containing N centers leads to 3N−6 true vibrational normal modes. As these are usually not localized motions of a small part of the molecule, assignment of the individual modes can, particularly in larger systems, be somewhat difficult. Several strategies can be used to facilitate the assignment of systems: vibrational band assignments are carried out by (1) constructing the IR absorption spectrum using Lorenzian line shape fitted to the experimental spectrum, or (2) animating Gaussian output vibrational bands using Gaussview and Hyperchem (Fig. 4, Table 3).

The optical activity of asymmetric molecules is explained when plane-polarized radiation passes through an active medium. The plane of the emergent plane-polarized radiation rotates by a given angle. The plane-polarized beam can be considered as a superimposition of two oppositely rotating circularly polarized components. The absorbance coefficient is defined as $\Delta\varepsilon = \varepsilon_L - \varepsilon_R$ [21]

Fig. 4 FTIR spectra decomposed theoretically for complex $[Zn(en)_3]Cl_2$
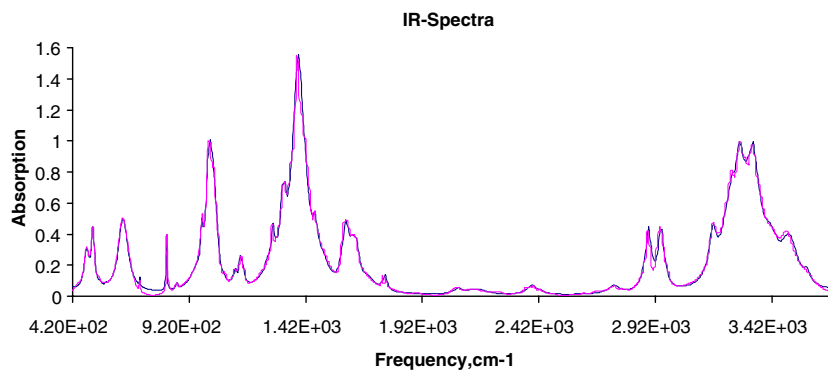
Table 3 Frequency (cm⁻¹) assignment of the Zn complex. *Be* Bending, *Ro* rocking, *Tw* twisting, *Sc* scissoring, *Str* stretching, *Wa* wagging. E, A, B, A_1, A_2 are irreducible representations of the corresponding D_3 and C_2 symmetry point groups. A scaling factor of 0.97 was used

No	Assignment	B3LYP/6–31G; Zn(en)₃Cl₂				B3LYP/6–31G; Zn(en)₃²⁺				
		Δ(λλλ)	Δ(λλδ)	Δ(λδδ)	Δ(δδδ)	Δ(λλλ)	Δ(λλδ)	Δ(λδδ)	Δ(δδδ)	Experimental
1	ZnCl₂,Be	51.1	41.9	40.8	48.8					
2	ZnCl₂,Be	51.1	47.3	42.2	48.8					
3	ZnCl₂,Be	76.7	58.1	51.7	57.9					
4	ZnCl₂,Be	76.7	74.2	55.7	57.9					
5	ZnCl₂,Str	95.5	88.6	82.4	71.3					
6	ZnCl₂,Str.	98.6	95.3	94.1	101.1					
7	ZnNC, Be	112.3	96.9	98.9	101.1	E, 42.1	B, 43.0	A, 50.8	E, 55.6	
8	ZnNC, Be	112.3	109.5	102.3	102.7	E, 42.1	A, 52.8	B, 51.9	E, 55.6	
9	ZnN₂, Tw	136.3	123.0	120.0	122.3	A₂, 64.4	B, 68.0	B, 63.5	A₂, 70.3	
10	ZnN₂, Tw	136.3	130.8	130.0	122.3	E, 71.0	A, 68.9	A, 70.2	E, 71.3	
11	ZnNC, Be	137.7	135.9	131.6	131.1	E, 71.0	B, 73.7	B, 73.7	E, 71.3	
12	ZnN₂, Tw	148.9	148.2	147.7	143.5	A₁, 72.0	A, 76.6	A, 85.1	A₁, 97.5	
13	ZnN₂, Wa	175.6	166.3	154.5	153.6	A₂,117.6	B, 124.5	B, 129.7	A₂,134.3	
14	ZnN₂, Wa	175.6	169.9	169.4	153.6	E, 142.2	B, 138.4	A, 130.6	E, 134.3	
15	ZnN₂, Wa	198.1	175.4	171.9	174.3	E, 142.2	A, 145.5	B, 147.3	E, 147.4	
16	ZnN₂, Str	198.1	192.1	173.6	174.3	E, 169.5	B, 161.0	B, 159.8	E, 166.0	
17	ZnN₂, Str	205.3	208.9	208.1	189.8	E, 169.5	A, 161.4	A, 149.4	E, 166.0	
18	ZnN₂, Str	211.8	209.6	209.8	215.8	A₁,173.7	A, 178.1	A, 179.7	A₁,183.6	
19	ZnN₂, Str	217.1	217.1	218.9	231.1	E, 200.2	A, 197.6	B, 196.2	E, 201.3	
20	ZnN₂, Str	217.1	227.3	233.7	231.1	E, 200.2	B, 205.0	A, 202.9	E, 201.3	
21	ZnN₂, Str	253.3	246.7	240.5	249.0	A₂,241.2	B, 239.6	B, 238.1	A₂,2 37.5	
22	NCC, Be	268.1	249.3	247.9	249.6	E, 258.4	A, 260.0	B, 257.0	E, 257.2	
23	NCC, Be	268.1	268.5	250.9	249.6	E, 258.4	B, 260.5	A, 257.8	E, 257.2	
24	NCC, Be	293.9	252.1	277.2	254.1	A₁,271.6	B, 270.0	A, 266.3	A, 265.8	
25	ZnN₂, Sc	385.2	383.9	388.5	393.1	E, 360.4	A, 356.7	B, 353.0	E, 353.6	
26	ZnN₂, Sc	385.2	388.9	391.1	393.1	E, 360.4	B, 359.0	A, 358.3	E, 353.6	
27	ZnN₂, Sc	407.7	408.9	413.2	417.2	A₁,383.2	A, 381.0	A, 383.6	A₁,3 92.2	
28	CH₂, NH₂, Ro	479.9	484.5	488.6	508.1	A₂,450.9	B, 453.7	B, 456.0	A₂,4 67.9	498
29	CH₂, NH₂, Ro	516.0	512.8	508.6	513.5	E, 480.7	B, 471.1	A, 469.0	E, 478.4	508
30	CH₂, NH₂, Ro	516.0	516.9	515.1	513.5	E, 480.7	A, 492.8	B, 487.0	E, 478.4	507
31	CH₂, NH₂, Ro	576.5	552.7	553.0	553.8	E, 504.6	B, 510.7	A, 519.3	E, 547.1	554
32	CH₂, NH₂, Ro	576.5	577.4	558.4	564.0	E, 504.6	A, 513.0	B, 531.9	E, 547.1	564
33	CH₂, NH₂, Ro	658.9	613.4	581.4	564.0	A₁,584.3	A, 570.0	A, 547.8	A₁,525.7	564
34	NH₂, Tw + CH₂, Ro	659.9	642.9	614.9	569.3	E, 604.3	B, 594.0	B, 572.1	E, 651.5	575
35	NH₂, Tw + CH₂, Ro	693.7	689.3	670.7	666.5	E, 604.3	A, 607.0	B, 629.2	E, 651.5	667
36	NH₂, Tw + CH₂, Ro	693.7	699.2	691.7	666.5	A₂,626.0	B, 644.5	A, 649.9	A₂,553.4	667
37	NC + CC, Str	856.5	853.7	853.4	853.4	E, 844.8	B, 840.0	A, 838.8	E, 838.7	853
38	NC + CC, Str	856.5	854.9	854.0	853.4	E, 844.8	A, 844.0	B, 839.9	E, 838.7	853
39	NC + CC, Str	861.2	858.9	856.5	855.8	E, 849.4	B, 848.0	A, 846.7	E, 846.7	856
40	NC + CC, Str	863.1	859.8	858.7	855.8	E, 849.4	A, 848.7	B, 848.0	E, 846.7	856
41	NC + CC, Str	863.1	861.2	858.9	857.0	A₁,850.8	A, 850.5	A, 849.8	A₁,849.2	860
42	NC + CC, Str	873.7	870.5	869.7	867.2	A₂,852.2	B, 853.1	B, 855.2	A₂,856.5	870
43	CH₂, Ro + NH₂, Tw	952.9	947.0	944.6	944.5	E, 953.6	A, 954.6	B, 954.9	E, 953.5	945
44	CH₂, Ro + NH₂, Tw	952.9	954.7	949.3	944.5	E, 953.6	B, 955.0	B, 955.5	E, 953.5	945
45	CH₂, Ro + NH₂, Tw	958.2	957.5	957.5	952.2	A₁,958.5	A, 958.8	A, 958.7	A₁,958.3	952
46	NC + CC, Str	1,017.0	1,010.5	1,006.2	1,006.8	E, 991.9	B, 992.7	B, 994.0	E, 996.0	1,007
47	NC + CC, Str	1,017.0	1,015.4	1,012.9	1,006.8	E, 991.9	A, 993.3	A, 994.2	E, 996.0	1,007
48	NC + CC, Str	1,032.9	1,028.7	1,028.5	1,029.5	E,1,002.7	B,1,001.1	B,1,000.7	E,1,001.0	1,029
49	NC + CC, Str	1,032.9	1,032.0	1,030.1	1,029.5	E,1,002.7	A,1,001.6	A,1,001.4	E,1,001.0	1,029
50	NC + CC, Str	1,033.5	1,032.6	1,031.7	1,031.6	A₂,1,003.5	B,1,002.7	B,1,002.0	A₂,1,001.0	1,031
51	NC + CC, Str	1,039.3	1,038.7	1,040.5	1,044.0	A₁,1,014.8	A,1,013.5	A,1,015.2	A₁,1,017.6	1,042
52	HCC + HNC, Be	1,061.0	1,057.4	1,058.2	1,055.6	A₂,1,067.3	B,1,068.0	A,1,068.4	A₂,1,086.0	1,055
53	HCC + HNC, Be	1,061.0	1,063.2	1,059.2	1,055.6	E, 1,075.8	B,1,074.5	B,1,074.3	E, 1,069.1	1,055

Table 3 (continued)

No	Assignment	B3LYP/6–31G; Zn(en)$_3$Cl$_2$				B3LYP/6–31G; Zn(en)$_3$$^{2+}$				
		$\Delta(\lambda\lambda\lambda)$	$\Delta(\lambda\lambda\delta)$	$\Delta(\lambda\delta\delta)$	$\Delta(\delta\delta\delta)$	$\Delta(\lambda\lambda\lambda)$	$\Delta(\lambda\lambda\delta)$	$\Delta(\lambda\delta\delta)$	$\Delta(\delta\delta\delta)$	Experimental
54	HCC + HNC, Be	1,061.7	1,073.7	1,078.5	1,086.7	E, 1,075.8	A,1,078.0	B,1,081.6	E, 1,069.1	1,085
55	NH$_2$, Wa	1,130.5	1,107.6	1,101.9	1,104.5	E,1,119.3	A,1,118.7	B,1,119.2	E, 1,122.1	1,107
56	NH$_2$, Wa	1,130.5	1,124.1	1,115.5	1,104.5	E,1,119.3	B,1,120.0	A,1,121.5	E, 1,122.1	1,110
57	NH$_2$, Wa	1,134.7	1,131.1	1,122.6	1,122.8	E,1,120.5	A,1,122.8	A,1,125.5	E, 1,129.7	1,122
58	NH$_2$, Wa	1,134.7	1,133.8	1,128.1	1,122.8	E,1,120.5	B,1,128.5	B,1,129.3	E, 1,129.7	1,122
59	NH$_2$, Wa	1,152.8	1,150.3	1,145.9	1,130.7	A$_1$,1,130.1	A,1,130.4	A,1,133.8	A$_1$,1,135.3	1,135
60	NH$_2$, Wa	1,175.5	1,167.3	1,155.6	1,139.7	A$_2$,1,143.8	B,1,141.0	B,1,140.1	A$_2$,1,143.4	1,145
61	HCC + HNC, Be	1,271.3	1,259.9	1,254.6	1,253.8	E, 1,278.8	A,1,279.1	A,1,280.2	E, 1,281.4	1,253
62	HCC + HNC, Be	1,271.3	1,270.4	1,260.4	1,253.8	E, 1,278.8	B,1,280.0	B, 1,282.2	E, 1,281.4	1,253
63	HCC + HNC, Be	1,275.9	1,274.9	1,272.6	1,265.8	A$_1$,1,284.9	A,1,285.7	A,1,285.4	A$_1$,1,284.0	1,265
64	CH$_2$ + NH$_2$, Tw	1,294.1	1,284.7	1,282.9	1,281.5	E, 1,294.8	B,1,294.6	B,1,295.3	E, 1,296.7	1,278
65	CH$_2$ + NH$_2$, Tw	1,294.1	1,294.7	1,284.3	1,281.5	E, 1,294.8	A,1,295.0	A,1,295.7	E, 1,296.7	1,280
66	CH$_2$ + NH$_2$, Tw	1,302.4	1,300.6	1,298.8	1,283.7	A$_1$,1,296.5	A,1,296.0	A,1,297.0	A$_1$,1,297.6	1,284
67	CH$_2$ + NH$_2$, Tw	1,338.4	1,322.9	1,318.9	1,317.8	E, 1,335.7	A,1,336.0	B,1,336.8	E, 1,338.1	1,320
68	CH$_2$ + NH$_2$, Tw	1,338.4	1,338.3	1,322.9	1,317.8	E, 1,335.7	B,1,336.7	A,1,338.0	E, 1,338.1	1,320
69	CH$_2$ + NH$_2$, Tw	1,345.0	1,343.4	1,341.7	1,324.4	A$_2$,1,338.2	B,1,339.2	B,1,338.6	A$_2$,1,338.6	1,332
70	CH$_2$, Wa	1,385.2	1,383.7	1,383.2	1,388.5	E, 1,398.8	A,1,398.6	B,1,399.3	E, 1,399.1	1,380
71	CH$_2$, Wa	1,385.2	1,385.3	1,388.9	1,388.5	E, 1,398.8	B,1,399.0	A,1,399.3	E, 1,399.1	1,390
72	CH$_2$, Wa	1,387.9	1,391.1	1,392.4	1,393.4	A$_2$,1,399.2	B,1,400.3	B,1,402.1	A$_2$,1,403.0	1,393
73	CH$_2$, Wa	1,392.6	1,392.3	1,392.8	1,394.5	E, 1,406.4	A,1,406.1	A,1,405.6	E, 1,406.2	1,395
74	CH$_2$, Wa	1,392.6	1,392.3	1,394.8	1,394.5	E, 1,406.4	B,1,406.2	B,1,406.5	E, 1,406.2	1,395
75	CH$_2$, Wa	1,392.9	1,396.4	1,398.1	1,398.8	A$_1$ 1,406.4	A,1,407.0	A,1,407.8	A$_1$,1,408.2	1,400
76	CH$_2$, Sc	1,497.3	1,497.9	1,498.9	1,500. 2	A$_1$,1,499.6	A,1,499.9	A,1,498.3	A$_1$,1,498.0	1,499
77	CH$_2$, Sc	1,497.9	1,498.2	1,499.8	1,500. 2	E, 1,500.1	A,1,500.0	A,1,499.4	E, 1,498.1	1,500
78	CH$_2$, Sc	1,497.9	1,498.9	1,499.8	1,500.8	E, 1,500.1	B,1,500.2	B,1,499.7	E, 1,498.1	1,500
79	CH$_2$, Sc	1,498.7	1,499.5	1,500.3	1,501.5	A$_2$,1,502.8	B,1,502.5	B,1,501.4	A$_2$,1,501.3	1,501
80	CH$_2$, Sc	1,499.9	1,499.5	1,500.9	1,501.5	E, 1,503.7	B,1,503.4	A,1,503.7	E, 1,501.3	1,501
81	CH$_2$, Sc	1,499.9	1,500.3	1,501.0	1,501.7	E, 1,503.7	A,1,503.8	B,1,503.8	E, 1,501.6	1,502
82	NH$_2$, Sc	1,665.4	1,656.5	1,654.7	1,659.3	A$_2$,1,651.2	B,1,651.0	B,1,654.2	A$_2$,1,661.9	1,660
83	NH$_2$, Sc	1,673.8	1,666.7	1,661.9	1,660.8	A$_1$,1,659.1	A,1,661.2	A,1,665.2	A$_1$,1,666.2	1,660
84	NH$_2$, Sc	1,688.6	1,676.8	1,664.1	1,660.8	E, 1,668.8	A,1,666.7	B,1,666.8	E, 1,666.2	1,660
85	NH$_2$, Sc	1,688.6	1,678.9	1,668.3	1,670.7	E, 1,668.8	B,1,667.6	A,1,667.5	E, 1,672.9	1,671
86	NH$_2$, Sc	1,693.4	1,688.2	1,683.7	1,670.7	E, 1,673.4	A,1,673.9	A,1,675.7	E, 1,673.6	1,671
87	NH$_2$, Sc	1,693.4	1,690.9	1,685.4	1,674.1	E, 1,673.4	B,1,675.6	B,1,676.7	E, 1,673.6	1,674
88	CH$_2$, Sym Str	2,942.5	2,941.2	2,940.3	2,939.0	A$_2$,2,982.8	B,2,981.2	A,2,981.8	A$_2$,2,982.7	2,940
89	CH$_2$, Sym Str	2,942.6	2,942.2	2,940.5	2,939.0	E, 2,983.1	B,2,981.4	B,2,981.8	E, 2,982.7	2,940
90	CH$_2$, Sym Str	2,942.6	2,942.3	2,940.9	2,939.3	E, 2,983.1	B,2,983.0	A,2,982.7	E, 2,982.8	2,940
91	CH$_2$, Sym Str	2,954.6	2,951.6	2,950.9	2,950.0	E, 2,983.2	A,2,983.2	B,2,982.8	E, 2,983.5	2,952
92	CH$_2$, Sym Str	2,954.6	2,954.3	2,951.5	2,950.0	E, 2,983.2	B,2,983.5	B,2,982.9	E, 2,983.5	2,952
93	CH$_2$, Sym Str	2,955.6	2,955.0	2,953.2	2,951.1	A$_1$,2,983.2	A,2,983.5	A,2,983.1	A$_1$,2,983.6	2,958
94	CH$_2$, Asym Str	2,999.5	2,983.0	2,981.9	2,980.5	E, 3,026.3	A,3,024.4	B,3,024.6	E, 3,024.8	2,950
95	CH$_2$, Asym Str	2,999.5	2,989.5	2,982.1	2,980.5	E, 3,026.3	B,3,025.9	A,3,024.7	E, 3,024.8	2,950
96	CH$_2$, Asym Str	2,999.7	2,989.7	2,986.5	2,980.8	A$_1$,3,026.5	A,3,026.0	A,3,025.4	A$_1$,3,025.0	2,952
97	CH$_2$, Asym Str	3,010.2	3,003.6	3,003.0	3,002.1	A$_2$,3,037.9	B,3,035.8	B,3,036.6	A$_2$,3,037.2	2,998
98	CH$_2$, Asym Str	3,010.6	3,009.5	3,003.1	3,002.1	E, 3,038.0	B,3,037.7	A,3,036.6	E, 3,037.2	3,020
99	CH$_2$, Asym Str	3,010.6	3,009. 7	3,006.4	3,002.2	E, 3,038.0	A,3,038.0	B,3,037.2	E, 3,037.2	3,020
100	NH$_2$, Sym Str	3,119.8	3,094.9	3,093.3	3,228.2	E, 3,354.1	B,3,353.4	B,3,352.5	E, 3,354.4	3,230
101	NH$_2$, Sym Str	3,119.8	3,102.3	3,100.8	3,228.2	E, 3,354.1	A,3,353.5	A,3,352.7	E, 3,354.4	3,230
102	NH$_2$, Sym Str	3,127.4	3,132.3	3,247.0	3,231.4	E, 3,354.8	B,3,354.0	B,3,353.4	E, 3,354.6	3,240
103	NH$_2$, Sym Str	3,127.4	3,138.8	3,249.6	3,231.4	E, 3,354.8	A,3,354.8	A,3,353.5	E, 3,354.6	3,239
104	NH$_2$, Sym Str	3,172.3	3,268.7	3,258.9	3,246.7	A$_2$,3,355.1	B,3,355.0	B,3,354.5	A$_2$,3,354.9	3,250
105	NH$_2$, Sym Str	3,178.2	3,270.9	3,261.3	3,249.1	A$_1$,3,356.5	A,3,355.6	A,3,354.7	A$_1$ 3,355.3	3,258
106	NH$_2$, Asym Str	3,420.6	3,418.9	3,418.6	3,442.6	E, 3,435.3	B,3,434.5	A,3,432.8	E, 3,436.4	3,440
107	NH$_2$, Asym Str	3,420.6	3,418.9	3,419.0	3,442.6	E, 3,435.3	A,3,434.8	B,3,433.6	E, 3,436.4	3,440

Table 3 (continued)

No	Assignment	B3LYP/6–31G; Zn(en)$_3$Cl$_2$				B3LYP/6–31G; Zn(en)$_3{}^{2+}$				Experimental
		$\Delta(\lambda\lambda\lambda)$	$\Delta(\lambda\lambda\delta)$	$\Delta(\lambda\delta\delta)$	$\Delta(\delta\delta\delta)$	$\Delta(\lambda\lambda\lambda)$	$\Delta(\lambda\lambda\delta)$	$\Delta(\lambda\delta\delta)$	$\Delta(\delta\delta\delta)$	
108	NH$_2$, Asym Str	3,421.4	3,419.9	3,441.4	3,443.0	E, 3,435.7	B, 3,435.8	A, 3,435.2	E, 3,436.9	3,441
109	NH$_2$, Asym Str	3,421.8	3,421.1	3,441.5	3,443.1	E, 3,435.7	A, 3,436.2	B, 3,435.2	E, 3,436.9	3,442
110	NH$_2$, Asym Str	3,421.8	3,446.6	3,443.9	3,443.1	A$_2$, 3,437.3	A, 3,437.3	B, 3,436.7	A$_2$, 3,437.0	3,442
111	NH$_2$, Asym Str	3,422.0	3,447.0	3,444.4	3,444.0	A$_1$, 3,437.7	B, 3,437.4	A, 3,436.9	A$_1$, 3,437.0	3,444

and the line shape is nearly Gaussian. The absorbance coefficient of the VCD is given by Eq. 1:

$$\Delta\varepsilon = \frac{2\sqrt{\ln 2}\,R\overline{v}}{2.296 \times 10^{-39}\sqrt{\pi}\,\Gamma_{1/2}}$$
$$\times \exp\left[4\ln(2)\left(\frac{\overline{v}-\overline{v}_0}{\Gamma_{1/2}}\right)^2\right] \quad (1)$$

Where R is the rotational strength and $\Gamma_{1/2}$ is the full width at the half height. Reading the rotational constant from the Gaussian output, and using the constant full line width of 20 cm^{-1} similar to the IR absorbance spectra, VCD absorption spectra can be constructed (Figs. 5, 6, 7).

When the complex, [Zn(en)$_3$]Cl$_2$, is due to the flipping of the C–C backbone in one of the ethylenediamine ligands from the δ to the λ form, the resulting $\Delta(\lambda\lambda\lambda)$ to $\Delta(\delta\lambda\lambda)$ conformational change reduces the symmetry to C$_2$. This type of conformational change, even if it does not move the N atom, can influence the electronic properties of the complex as a change in the Zn–N–C angle can influence the direction of the bonding N orbitals. Small amounts of "bent bonding" were required in the interpretation [22] of the circular dichroism of [Zn(en)$_3$]Cl$_2$.

The vibrations appeared in groups of three or six depending on ring deformations or the stretching or bending activities of functional groups such as CH$_2$ or NH$_2$. The major frequency shifts among different conformations are in the 400–700 cm^{-1} area, areas of CH$_2$+NH$_2$ rock and CH$_2$ twist+NH$_2$ rock, and NH$_2$ and CH$_2$ scissoring occur also in the area 1,600–1,700 cm^{-1}. Almost all of the H atoms in the bending area are moving, therefore assignments are rather uncertain; however, the most dominant and active modes are assigned. Unlike functional frequencies, the skeleton frequencies for different conformers are shifted, as expected, and some appear with different intensities.
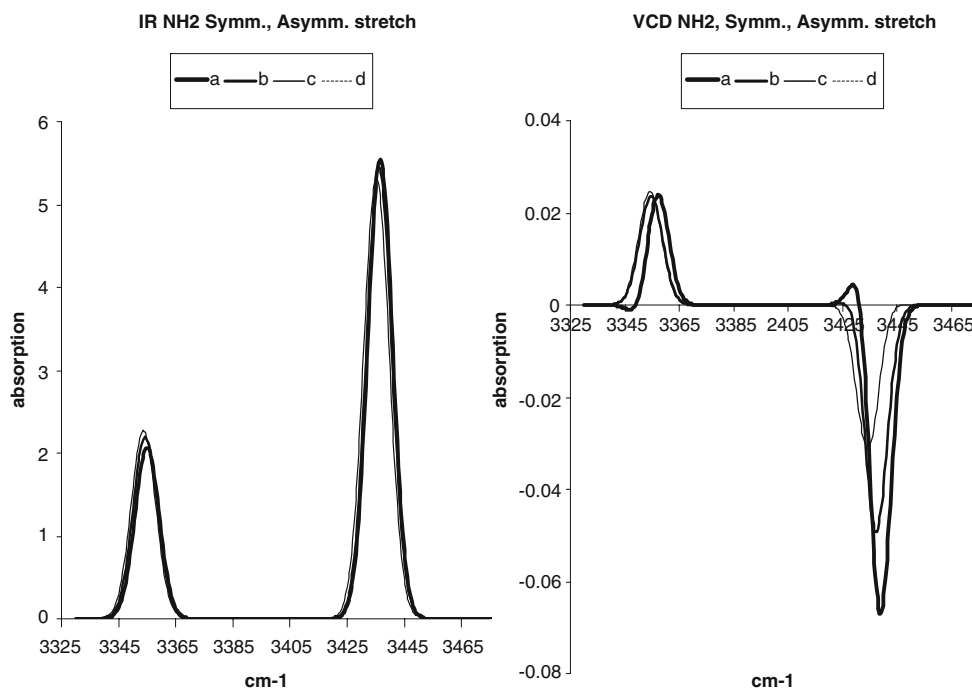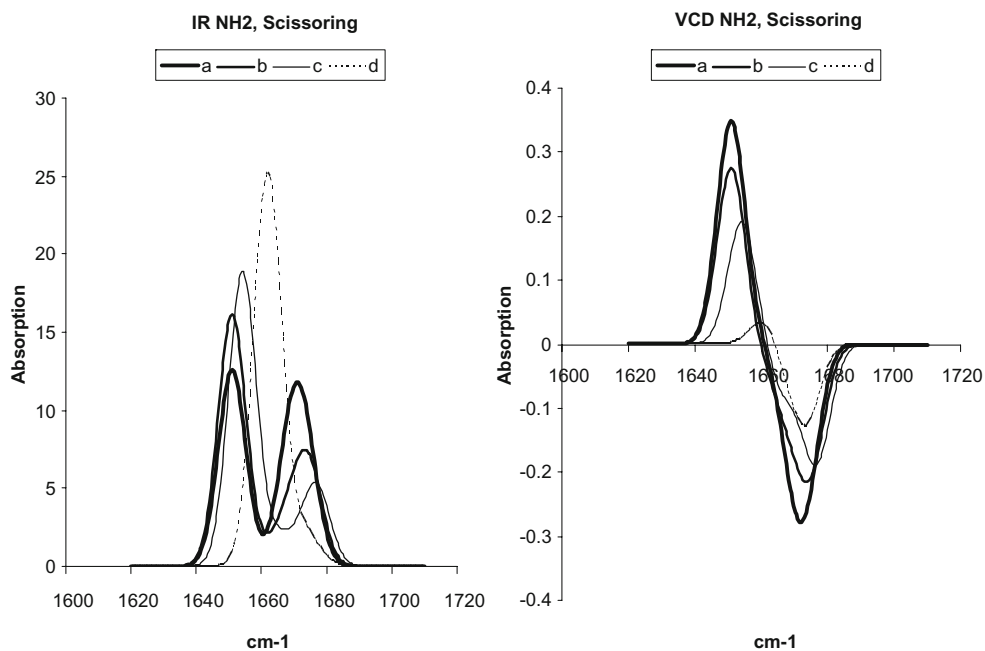

Fig. 5 Infrared and vibrational dichroism spectroscopy (VCD) NH$_2$ symmetry and asymmetry stretching modes

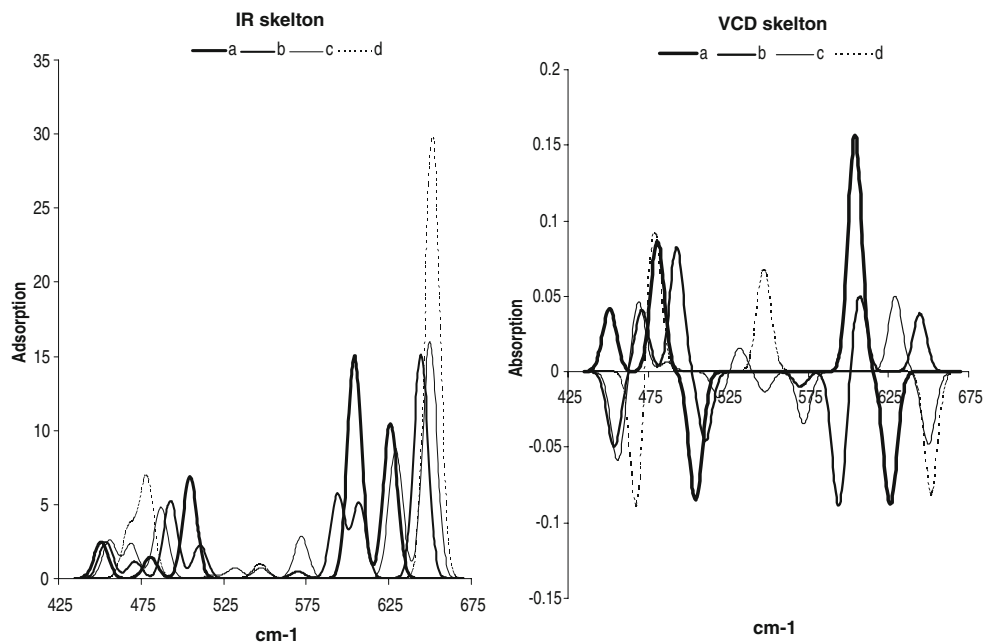**Fig. 6** Infrared and VCD of NH₂ scissoring modes

Discussion

The VCD measurements were more accurate than the corresponding IR experiments due to the differences in experimental settings illustrated in Eq. 2; whereas alignment errors accumulate in IR, they cancel each other out in VCD.

$$\text{IR};\ \Delta\varepsilon = \varepsilon_L + \varepsilon_R$$
$$\text{VCD};\ \Delta\varepsilon = \varepsilon_L - \varepsilon_R \qquad (2)$$

In the geometry optimization, the two dihedral angles H–N–Zn–X and H–C–N–H played the major roles from one conformation to the other. These two angles can be considered equally as H–N–C and H–C–N out-of-plane bending modes, and it is expected that a combination of CH_2 and NH_2 bending would be affected by the conformational change. IR vibrational modes for all four conformations except NH_2 wagging at 1,120 and 1,142 cm⁻¹, HCC+HNC bending at 1,070 cm⁻¹ and the 400–700 cm⁻¹ area appear at the same frequencies and intensities, but VCD band polarization changes, giving a detailed structural mode leading to easy conformational distinction.

Fig. 7 Infrared and VCD Zn-N skeleton modes

Different areas of the $Zn(en)_3^{2+}$ complex were magnified to investigate the behavior of the vibrational modes involved with respect to right and left polarizations. NH_2 asymmetry stretching at 3,436 cm^{-1} for the conformations $\Delta(\lambda\lambda\lambda)$, $\Delta(\lambda\lambda\delta)$, $\Delta(\lambda\delta\delta)$ to $\Delta(\delta\delta\delta)$ lost right polarization intensities by about one-quarter and gained left activity for each step of deformational change. NH_2 symmetry stretching at 3,355 cm^{-1} for all conformations appeared at the same frequency and intensity for both IR and VCD, suggesting an invariant response to polarized light (Fig. 5).

CH_2 asymmetry stretching at 3,026 and 3,036 cm^{-1} for $\Delta(\lambda\lambda\lambda)$ conformation is right polarized, whereas CH_2 symmetry stretching at 2,983 cm^{-1} is left polarized. The $\Delta(\lambda\lambda\delta)$ structure is losing about half of the corresponding intensity and gaining opposite polarization, and this situation is continued for the $\Delta(\lambda\delta\delta)$ complex and ends with the converse situation for the $\Delta(\delta\delta\delta)$ conformation.

Unlike in Fig. 5, there is no frequency shift from one isomer to another for the NH_2 scissoring bands at 1,651 cm^{-1} and 1,673 cm^{-1}. These two bands are in fact a combination of six (1,651, 1,659, 1,669, 1,669, 1,673 and 1,673 cm^{-1}) transitions. The intensity of the outer bands decreases and the inner bands gain in intensity with each conformational change from $\Delta(\lambda\lambda\lambda)$ to $\Delta(\delta\delta\delta)$ complexes, and finally only one strong band appears at 1,665 cm^{-1} (Fig. 6). Whereas in VCD, the band at 1,651 cm^{-1} from left polarization dies out in a step of one-quarter, the band at 1,670 cm^{-1} from right polarization dies out at a slower rate. The same behavior as CH_2 stretching is seen for CH_2 scissoring at 1,502 cm^{-1}.

NH_2 wagging at 1,120 cm^{-1} is shifted to a higher frequency by a step of about 3 cm^{-1} from $\Delta(\lambda\lambda\lambda)$ to $\Delta(\delta\delta\delta)$, and HCC+HNC bending at 1,076 cm^{-1} shifts to a lower frequency. Shifting frequency and polarization results in the complex behavior of the VCD spectra. CH_2 wagging at 1,402 cm^{-1} has a similar trend as the conformation changes shown in Table 3.

NH_2+CH_2 twisting at 1,294 and 1,338 cm^{-1} and C–C+C–N stretches occur in area 825–1,025 cm^{-1}. The frequency shift is about 1 cm^{-1} for each step of the conformational change but, for example, the optical activity of the band at 1,294 cm^{-1} of the $\Delta(\lambda\lambda\lambda)$ conformer from right polarization loses about 50% of its intensity compared to the $\Delta(\lambda\lambda\delta)$ conformer and changes to left polarization for $\Delta(\lambda\delta\delta)$ and $\Delta(\delta\delta\delta)$ (Table 3).
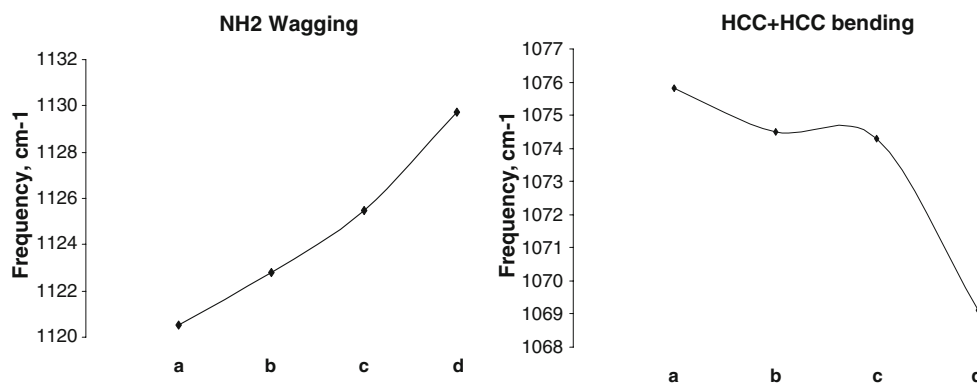
Optical activity does not change in the area 175–400 cm^{-1} of the Zn–N stretch, but the intensity changes from $\Delta(\lambda\lambda\lambda)$ to $\Delta(\delta\delta\delta)$. In the skeleton area 400–675 cm^{-1} (Fig. 7), intensity changes, shifting and overlapping of frequencies provide interesting features due to the appearance of many transitions occurring within a small area.

A combination of NH_2 and CH_2 twisting and rocking modes occur in the 400–700 cm^{-1} region, and we expect some frequency shifts among different isomers. The variation of ν_{22} and ν_{29} with the conformation change for $\Delta(\delta\delta\delta)$, $\Delta(\delta\delta\lambda)$, $\Delta(\delta\lambda\lambda)$ and $\Delta(\lambda\lambda\lambda)$ are plotted in Fig. 8.

Conclusion

The calculated relative conformational energies of [Zn(en)$_3$]Cl$_2$ (Table 2) fall within 0.17 kcal/mol. The relative conformational energy of $\Delta(\lambda\lambda\lambda)$=0.0 kcal/mol; this conformer has the lowest energy. The next highest energy isomer is $\Delta(\delta\delta\delta)$ at 0.12 kcal/mol. These two conformers occur in two-thirds of reported structures, presumably because these are the configurations most easily stabilized by hydrogen bonds. Conversely, the single examples of the $\Delta(\delta\delta\lambda)$ and $\Delta(\delta\lambda\lambda)$ configurations indicate that these represent higher energy isomers. Furthermore, the large number of strong hydrogen bonds found in the $\Delta(\delta\delta\delta)$ structure support this assignment. The results for $\Delta(\delta\delta\lambda)$ and $\Delta(\delta\lambda\lambda)$ are more ambiguous. Their relative rarity warrants placing these configurations as the second highest energy isomer. We thus propose the following order for the relative conformational energies of the four unique Δ configuration isomers: $\Delta(\lambda\lambda\lambda)$ <($\Delta\delta\delta\delta$) <$\Delta(\delta\lambda\lambda)$ <$\Delta(\delta\delta\lambda)$

Fig. 8 Variations of ν_{22} and ν_{29} with conformation change

References

1. Bernhardt PV, Riley MJ (2003) Aust J Chem 56:287–291. doi:10.1071/CH03023
2. Palmer RA, Yang MC-L (1978) J Am Chem Soc 100:3780. doi:10.1021/ja00480a021
3. Neil D, Riley MJ, Kennard CHL (1997) Acta Crystallogr Sec B 701:53
4. Freedman TB, Cao X, Young DA, Nafie LA (2002) J Phys Chem 106:3560–3565
5. Autschbach J, Jorge FE, Ziegler T (2003) Inorg Chem 42:2867–2877. doi:10.1021/ic020580w
6. Cullen DL, Lingafelter EC (1970) Inorg Chem 9:1858. doi:10.1021/ic50090a016
7. Whuler A, Brouty C, Spinat P, Herpin P (1976) Acta Crystallogr B 32:194. doi:10.1107/S0567740876002574
8. Spek AL (2003) J Appl Crystallogr 36:7–13. doi:10.1107/S0021889802022112
9. Corey EJ, Bailar JC Jr (1959) J Am Chem Soc 81:2620. doi:10.1021/ja01520a006
10. Raymond KN, Corfield PWR, Ibers JA (1968) Inorg Chem 7:842. doi:10.1021/ic50062a051
11. Cramer RE, Van Doorne W, Huneke JT (1976) Inorg Chem 15:529. doi:10.1021/ic50157a009
12. Gollogly JR, Hawkins CJ, Beattie JK (1971) Inorg Chem 10:317. doi:10.1021/ic50096a020
13. Gaussian 03, Revision B.01, Frisch MJ, Trucks G W, Schlegel HB, Scuseria GE, Robb MA, Cheeseman JR, Montgomery JA, Jr. Vreven T, Kudin KN, Burant JC, Millam JM, Iyengar SS, Tomasi J, Barone V, Mennucci B, Cossi M, Scalmani G, Rega N, Petersson GA, Nakatsuji H, Hada M, Ehara M, Toyota K, Fukuda R, Hasegawa J, Ishida M, Nakajima T, Honda Y, Kitao O, Nakai H, Klene M, Li X, Knox J. E, Hratchian HP, Cross JB, Adamo C, Jaramillo J, Gomperts R, Stratmann RE, Yazyev O, Austin AJ, Cammi R, Pomelli C, Ochterski JW, Ayala PY, Morokuma K, Voth GA, Salvador P, Dannenberg JJ, Zakrzewski VG, Dapprich S, Daniels AD, Strain MC, Farkas O, Malick DK, Rabuck AD, Raghavachari K, Foresman JB, Ortiz JV,Cui Q, Baboul AG, Clifford S, Cioslowski J, Stefanov BB, Liu G, Liashenko A, Piskorz P, Komaromi I, Martin RL, Fox DJ, Keith T, Al-Laham MA, Peng CY, Nanayakkara A, M, Gill PMW, Johnson B, Chen W, Wong MW, Gonzalez, C, Pople JA (2003) Gaussian, Pittsburgh PA
14. Kohn W, Sham LJ (1965) Phys Rev 140:A1133. doi:10.1103/PhysRev.140.A1133
15. Vosko SH, Wilk L, Nusair M (1980) Can J Phys 8:12001
16. Becke AD (1988) Phys Rev A 38:3098. doi:10.1103/PhysRevA.38.3098
17. Lee C, Yang W, Parr RG (1988) Phys Rev B 37:785. doi:10.1103/PhysRevB.37.785
18. Cramer RE, Huneke JT (1978) Inorg Chem 17:365. doi:10.1021/ic50180a038
19. Cramer RE, Huneke JT (1975) Inorg Chem 14:2565. doi:10.1021/ic50152a060
20. Pavkovic SF, Meek DW (1965) Inorg Chem 4:1091. doi:10.1021/ic50030a001
21. Cheeseman JR, Frisch MJ, Devlin FJ, Stephens PJ (1996) Chem Phys Lett 211:252
22. Bridgeman AJ, Jupp KM, Gerloch M (1994) Inorg Chem 33:5424–5429. doi:10.1021/ic00102a013